Reduction of unbalanced magnetic forces in planar linear actuators

Florian Poltschak[a], Markus Speletz[a]

[a] JKU Hoerbiger Institute for Smart Actuators, Johannes Kepler University, Altenbergerstrasse 69, 4040 Linz, Austria, florian.poltschak@jku.at

***Abstract*—To reach a high axial thrust force density with planar linear motors slotted designs have advantages compared to the common air-gap winding topologies. Combined with a permanent magnet excitation compact solutions can be designed, which exhibit a significant force perpendicular to the direction of movement. Even with double sided topologies a destabilizing stiffness remains. This force adds up an extra load on the bearings and can significantly limit their life-time especially when bush bearings are applied.**
This paper introduces a concept to actively compensate for the permanent magnet induced bearing load. The potential and limits are analyzed based on a planar linear actuator with E-shaped stator cores and a four phase winding. It is outlined how an integrated active bearing force compensation can be reached for the complete axial stroke even with simple conventional actuator layouts. This method can (i) significantly reduce wear and thus improve lifetime and (ii) reduce the size of the mechanical bearings.
The system simulation results are validated with measurements of a prototype system.

I. Introduction

Many linear actuators and motors in industrial applications use an air-gap winding topology with a permanent magnet (PM) excitation. This reduces forces perpendicular to the direction of motion, but also limits the thrust force for a given PM volume. Thus usually a slotted stator topology is selected when the focus lies on high thrust force density. With symmetric planar or tubular designs unwanted forces perpendicular to the direction of movement can be reduced or ideally canceled. However most linear bearing solutions exhibit wear and the unbalanced magnetic forces lead to an excentric position of the mover and hence accelerated wear. Consequently the increased friction deteriorates efficiency and bearing lifetime. The effect of asymmetries resulting from manufacturing tolerances on unbalanced forces have been analyzed in [1] for rotational machines.
When the reduction of bearing forces of linear motors is discussed in literature two main force sources can be distinguished. Both are perpendicular to the direction of movement. The first is the gravity or load force compensation and the second the reduction of the unbalanced magnetic forces. The solutions of gravity compensation range from passive systems where PMs generate attractive forces counteracting gravity [2] to actives bearing-less systems [3].
The potential of reducing unbalance forces by design has been investigated in [4] for a doubly salient PM linear motor.

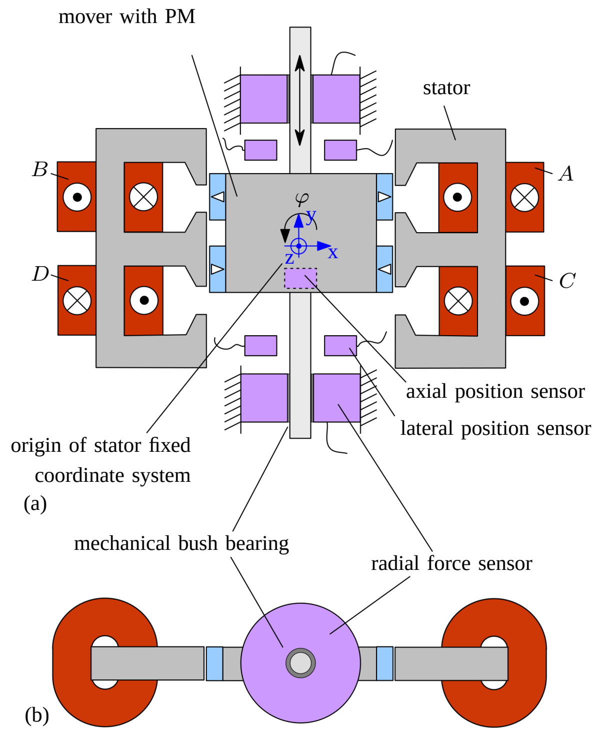

Figure 1. (a) Top view and (b) front view of the investigated linear actuator system with 4 phases labeled with A-D.

Reducing unbalanced magnetic forces perpendicular to the direction of movement in a given design planar linear actuator requires an active force compensation control. For core-less linear motors a method has been proposed in [5] by adding a second three phase winding system to gain some degree of freedom to compensate for parasitic forces and torques. The potential of reducing the undesired bearing forces of a slotted translational actuation system with a two phase winding is analyzed in [6]. It shows a significant rise in bearing lifetime. Still, it is not possible to cancel both bearing forces independently of the position of the mover. Especially for a short stroke operation next to the center region of the stator the force reduction capability is poor.

The objective of this paper is to further extend the reduction of the unbalanced magnetic forces by applying a 4-phase winding. This allows canceling both bearing force components

independent of the mover position. Imagine a reciprocating operation of such a system that could be used for example to drive a free piston compressor. Thus, for example, a dry running linear bearing will be available in the system but must not be exposed to the large unbalanced PM forces resulting from the magnetic actuator itself. Reducing the forces will reduce the bearing length and thus the length and mass of the mover. As a mechanical bearing will be still in place, there is no need to apply active magnetic bearings or a bearing-less motor design and the existing magnetic circuit of the linear actuator can be used to integrate the bearing force compensation.
The proposed force reduction is analyzed in simulation and validated with measurements on a test rig.

II. System model

All symbols to describe the system model and force compensation strategy are defined in Tab. I.

A. System layout

The system layout is given in Fig. 1. It features a two-sided planar E-shaped stator with two coils on each side, one for each phase. The planar mover is mounted to an axle with two PM on each side. With the mover in exact centered position the lateral forces disappear. External forces are assumed only to act along the y-axis. The actuator is designed to show a constant force-to-current ratio in the y-direction without cogging forces for a stroke $s = \pm 5mm$ around the center position. The main system dimensions are given in Tab. II.

Any eccentricity or wear in the x-direction causes an imbalance of the attractive forces. Two radial force gauges are applied to measure the resulting bearing forces. Additionally the axial and lateral position of the axis are measured to determine the axial mover position and its eccentricity and tilting angle.

B. Wear of linear bush bearings

Compensating for bearing forces of linear drives may come into focus for different reasons. Especially for integrated systems requirements like a small system size, minimum weight and low production costs which result in wide tolerances are likely to result in the need for low cost dry running bearings. On the contrary high performance requirements and a high overall system efficiency may as well result in the need for dry running bearings made from durable material. In any case, wear limits the lifetime of the bushings. In this context, the radial wear w is equivalent to an eccentricity of the mover in the x-direction. Assuming an actuator with an oscillating motion along the y-axis, a mean mover velocity v_m in the y-direction and a mean bearing pressure p_m in the x-direction can be defined. The differential equation for the wear [6] w is deduced empirically as

$$\dot{w}(t) = K_0 p_m(t) v_m, \tag{1}$$

the wear coefficient K_0 has the unit $\mathrm{ms}^2/\mathrm{kg}$. This wear parameter is a material property of the bushing.

Table I
Table of symbols.

symbol	description
$\mathbf{B}$	transformation matrix between bearing and mover forces
d	distance between bearings
d_b	outer diameter of bush bearing
h_b	length of bush bearing
F_{b1}, F_{b2}	bearing forces of bearing 1 or 2
F_x	force normal to air gap
F_y	thrust force
$\mathbf{i}$,$\mathbf{i}_c$	coil and phase current vector
i_A, i_B, i_C, i_D	currents of coils A to D
i_1, i_2, i_3	phase currents
k_{**}	stiffness in direction $* = x$,y,φ
$\mathbf{k}_q$	stiffness matrix
K_0	wear coefficient
$\mathbf{K}_m$	(pseudo-) inverse of $\mathbf{M}_L$
m	number of phases
$\mathbf{M}$	mass matrix
$\mathbf{M}_C$	matrix of constant forces
$\mathbf{M}_L$	matrix of force coefficients proportional to the current
$\mathbf{M}_Q$	matrix of force coefficients quadratic to the current
p_m	mean bearing pressure
$\mathbf{q}$	generalized coordinate vector
$\mathbf{Q}, \mathbf{Q}_F, \mathbf{Q}_l$	generalized forces on the mover
s	stroke in axial direction
t	time
T_z	torque along z axis
$\mathbf{V}$	phase connection matrix
v_m	mean bearing velocity
w	wear
x	mover position normal to air gap
y	mover position in axial direction
z	coordinate normal to x/y plane
φ	rotational angle along z-axis

It is assumed that all forces acting on the bearing are negligible compared to the resulting passive PM forces perpendicular to the direction of motion. Hence, the mean bearing pressure

$$p_m(t) = f(w(t)) \tag{2}$$

is a function of the wear (eccentricity) of the mover.
For the symmetrical electromagnetic actuator investigated, the forces perpendicular to the direction of motion can be approximated to change proportionally with the eccentricity or wear. The linear dependency is defined by the dominating stiffness k_{xx}. This leads to the expression

$$p_m(t) = \frac{k_{xx} w(t)}{2 h_b d_b \pi / 3} \tag{3}$$

Table II
MAIN SYSTEM DIMENSIONS.

parameter	value	unit
width (x direction)	10	mm
length(y direction)	10	mm
height(z direction)	15	mm
mover length	40.5	mm
air gap width	1	mm
total axial stroke	16	mm
distance of bearings	258	mm

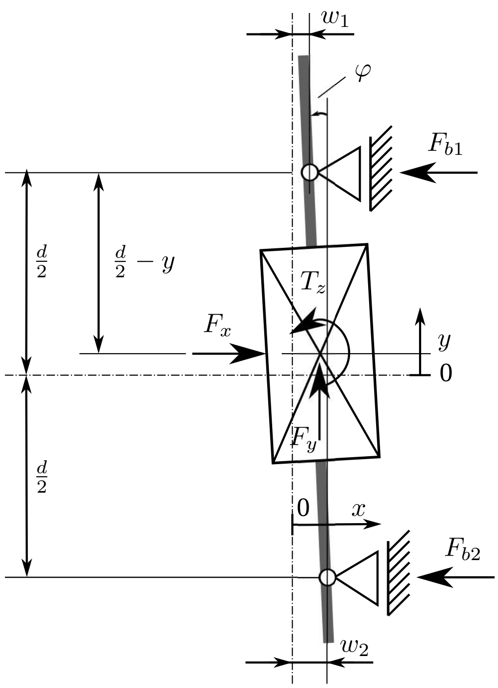

Figure 2. Model of static bearing forces under the influence of eccentricity and tilting.

for the mean bearing pressure. Both bearing rings have the same geometric dimensions of length h_b and outer diameter d_b. It is assumed that each ring bears only on one third of its circumferential surface. Given an inevitable initial eccentricity of w_0, the wear is:

$$w(t) = w_0 e^{\frac{3K_0 k_{xx} t v_m}{2 d_b h_b \pi}}. \tag{4}$$

From (4) follows that for fixed geometrical dimensions of the bearing rings the stiffness k_{xx} directly influences the lifetime

$$t_{\text{life}} = \frac{2 d_b h_b \pi \ln\left(\frac{w_{max}}{w_0}\right)}{3 K_0 k_{xx} v_m} \tag{5}$$

of the bearing, which reaches the end of its life when w reaches w_{max}.
Different initial eccentricities w_{10} and w_{20} of bearings 1 and 2, respectively, result according to (4) in different eccentricities w_1 and w_2. The definition of this wear and the resulting forces are visualized in Fig. 2.

C. Bearing forces

According to Fig. 2, the equilibrium of the bearing forces F_{b1}, F_{b2} and the force F_x resulting from eccentricities in the x-direction

$$F_{b1}(y) + F_{b2}(y) = F_x(y) \tag{6}$$

and the torque equilibrium

$$0 = F_{b2}(y) d + T_z(y) - F_x(y) \left(\frac{d}{2} - y\right) \tag{7}$$

yield

$$F_{b1}(y) = \frac{F_x(y)(d + 2y) + 2T_z(y)}{2d} \tag{8}$$

$$F_{b2}(y) = \frac{F_x(y)(d - 2y) - 2T_z(y))}{2d} \tag{9}$$

with the distance d between the two bearings. The torque T_z and the force F_x both depend on y and act on the center of the mover (Fig. 2).

III. DYNAMIC SYSTEM MODEL

The generalized forces

$$\mathbf{Q}_F = \begin{bmatrix} F_x \\ F_y \\ T_z \end{bmatrix} \tag{10}$$

on the mover with respect to $\mathbf{q} = [x, y, \varphi]^T$ result from the actual bearing forces and the external load. This results in the definition of forces in the form

$$\mathbf{Q}_F = \text{diag}(\mathbf{i}) \mathbf{M}_Q \mathbf{i} + \mathbf{M}_L \mathbf{i} + \mathbf{M}_C \tag{11}$$

with diag($\mathbf{i}$) defining the diagonal matrix of the phase currents. The term $\mathbf{M}_Q$ and $\mathbf{M}_L$ comprise the coefficients quadratic respectively proportional to the coil currents, and the term $\mathbf{M}_C$ the coefficients independent of the currents. The vector $\mathbf{i}$ has the dimension $m \times 1$, with m denoting the number of phases.
If linearity with respect to the currents is assumed and all terms of higher order with respect to $\mathbf{i}$ are ignored (11) can be simplified to

$$\mathbf{Q}_F = \mathbf{M}_L \mathbf{i} + \mathbf{M}_C. \tag{12}$$

This approximation is valid for small changes in the bearing eccentricities and has been confirmed by simulation and measurements. The nonlinear behavior in the direction of motion y is covered using a look-up table for this dimension. The linear model can now be expressed as

$$\mathbf{Q} = \mathbf{M}_L \mathbf{i} = \mathbf{Q}_F - \mathbf{M}_C. \tag{13}$$

The entries of the matrices $\mathbf{M}_L$ and $\mathbf{M}_C$ are calculated in a 2D finite element (FE) analysis of the system. Fig. 3 shows the simulation result of $\mathbf{M}_C$ with respect to the mover position y.

Assuming current control, a model based on the applied phase currents can be derived. When compensating for the

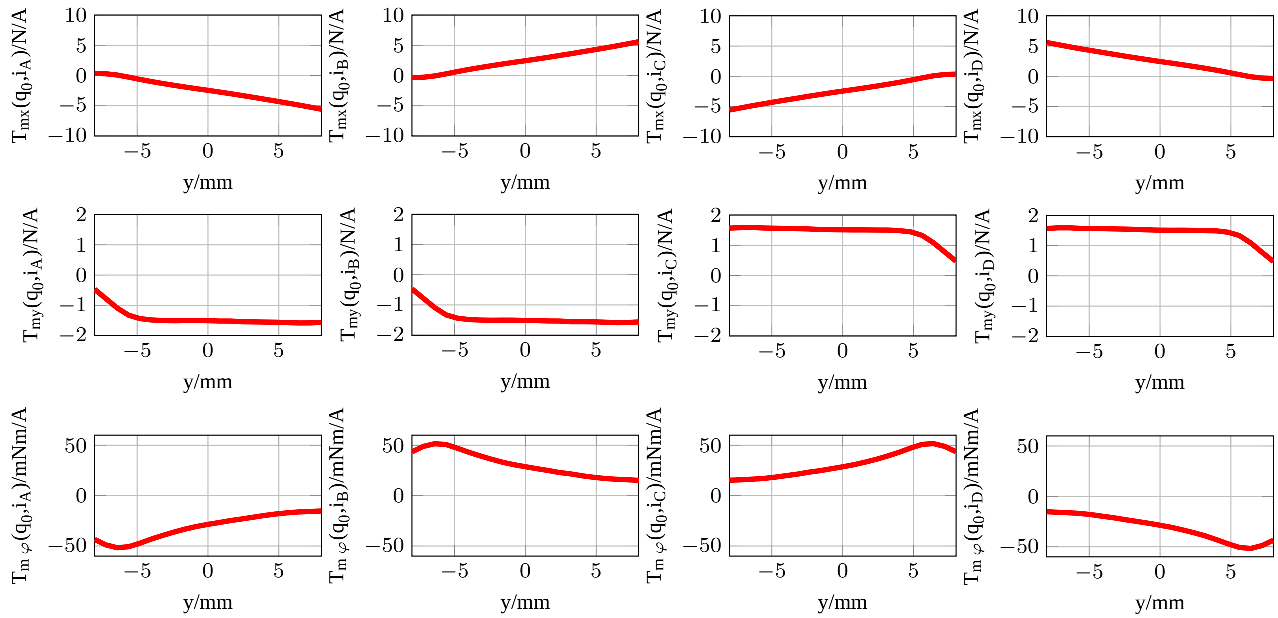

Figure 3. The simulation result of the $\mathbf{M}_L$-matrix shows the capability to generate bearing (x- and φ directions) and thrust (y-direction) forces in all positions.

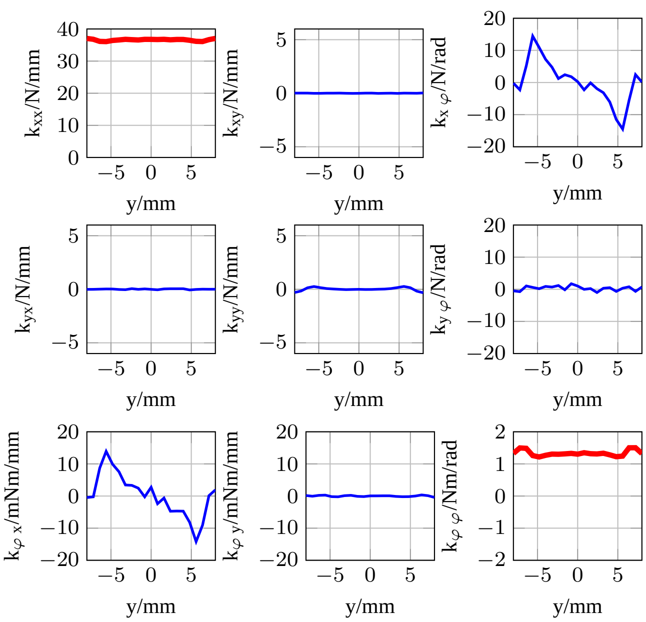

Figure 4. The simulation of the not energized system with respect to the axial stroke results is a symmetric stiffness matrix. The two significant entries are marked with bold red lines.

bearing forces the mover of the linear actuator is intended to be operated near the initial position

$$\mathbf{q}_0 = [x(w_{10}, w_{20}), y, \varphi(w_{10}, w_{20})]^T, \tag{14}$$

with w_{10} and w_{20} being the bearing position resulting from the initial eccentricities. The motion along the y-axis is valid for the full stroke as long as the assumption of proportionality to the current holds true.

Thus, at the point $\mathbf{q}_0$ the equation of motion

$$\mathbf{M}\ddot{\mathbf{q}} = \mathbf{Q}_F - \mathbf{Q}_l \tag{15}$$

with the generalized mass matrix $\mathbf{M}$ and the generalized load force $\mathbf{Q}_l(x_0, y, \varphi_0) = [0, F_{ly}, 0]^T$ can be developed into a Taylor series. Assuming that the system is at a stationary point of operation at the location $\mathbf{q}_0$, the current $\mathbf{i}_0(\mathbf{q}_0)$ is required to compensate for the load force F_{ly}. If the initial position cannot be measured, the initial wear can be assumed to zero with $\mathbf{i} = \mathbf{0}$ and $\mathbf{q}_0 = [x_0, y, \varphi_0]^T$. Ignoring all terms with a higher order than one results for this point of operation in

$$\begin{aligned}\mathbf{M}\ddot{\mathbf{q}} = &\left.\frac{\partial(\mathbf{M}_L\mathbf{i})}{\partial\mathbf{q}}\right|_{x_0,y,\varphi_0,\mathbf{i}_0}\mathbf{q} + \left.\frac{\partial\mathbf{M}_C}{\partial\mathbf{q}}\right|_{x_0,y,\varphi_0,\mathbf{i}_0}\mathbf{q}+ \\ &+\mathbf{M}_L\left(x_0, y, \varphi_0\right)\mathbf{i} + \left.\frac{\partial\mathbf{M}_C}{\partial\mathbf{i}}\right|_{x_0,y,\varphi_0}\mathbf{i}.\end{aligned} \tag{16}$$

The term $\mathbf{M}_C$ is per definition independent of the current $\mathbf{i}$, and the term $\mathbf{M}_L\mathbf{i}$ can be seen as approximately independent of x and φ. With the stiffness matrix

$$\mathbf{k}_q(y) = \left.\frac{\partial\mathbf{M}_C}{\partial\mathbf{q}}\right|_{x_0,y,\varphi_0,\mathbf{i}_0} \tag{17}$$

and $\mathbf{M}_{L0}(y) = \mathbf{M}_L(x_0, y, \varphi_0)$ the equation of motion in (16) can be simplified to

$$\mathbf{M}\ddot{\mathbf{q}} = \mathbf{k}_q\left(y\right)\mathbf{q} + \mathbf{M}_{L0}\left(y\right)\mathbf{i}. \tag{18}$$

Within the defined stroke of $y = \pm 5\,\mathrm{mm}$ the simulated stiffness matrix of the prototype system

$$\begin{aligned}\mathbf{k}_q(y) = &\begin{bmatrix} k_{xx} & k_{xy} & k_{x\varphi} \\ k_{yx} & k_{yy} & k_{y\varphi} \\ k_{\varphi x} & k_{\varphi y} & k_{\varphi\varphi}\end{bmatrix} = \\ = &\begin{bmatrix} 38\,\mathrm{N/mm} & 0 & 3y\,\mathrm{N/rad/mm} \\ 0 & 0 & 0 \\ 3y\,\mathrm{Nm/m/mm} & 0 & 1.3\,\mathrm{Nm/rad}\end{bmatrix}.\end{aligned} \tag{19}$$

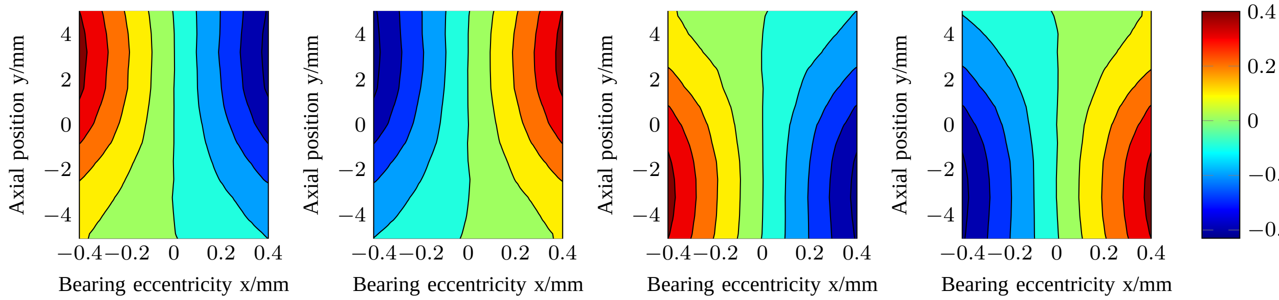

Figure 5. Simulation of the required bearing force compensation current in relation to the systems rated current for a bearing eccentricity $w_1 = w_2 = x$ and the axial position y. The figure shows from left to right the relative compensation currents for the coils A to D .

is visualized in Fig. 4. It shows two significant entries in the main diagonal representing the stiffness in x-direction and the rotation around the z-axis. Both are independent of the axial mover position. Most of the coupling terms vanish, except the coupling between the x and φ coordinates. These stiffness parameters ($k_{x\varphi}$ and $k_{\varphi x}$) depend approximately linear on the axial mover position y and result from the stator slotting. However with the mechanical limitations of the prototype system the tilting angle φ cannot exceed $0.45\,°$. Hence all coupling terms in $\mathbf{M}_C$ can be ignored.

IV. Bearing force reduction

A. System inversion

From the six degrees of freedom of the rigid body motion three degrees of freedom are actively controlled: (i) the axial motion in y-direction, (ii) the force in x-direction and (iii) the torque in φ-direction. All other degrees of freedom are stabilized passively by choosing the shape of the magnetic circuit or with the mechanical bearings.
According to (12) the bearing forces $\mathbf{F}_b$ and the desired axial force F_y can be written in the form

$$\mathbf{F}_b = \begin{bmatrix} F_{b1} \\ F_{b2} \\ F_y \end{bmatrix} = \mathbf{B} \begin{bmatrix} F_x \\ F_y \\ T_z \end{bmatrix} = \mathbf{B} \cdot \mathbf{M}_L \cdot \mathbf{i} + \mathbf{B} \cdot \mathbf{M}_C \qquad (20)$$

with the transformation matrix

$$\mathbf{B} = \begin{bmatrix} \frac{1}{2} + \frac{y}{d} & 0 & \frac{1}{d} \\ \frac{1}{2} - \frac{y}{d} & 0 & -\frac{1}{d} \\ 0 & 1 & 0 \end{bmatrix} \qquad (21)$$

that transforms the desired bearing (9) and axial forces to the mover coordinate system. $\mathbf{F}_b$ is nonlinear in y because $\mathbf{B}$, $\mathbf{M}_L$ and $\mathbf{M}_C$ depend on the position y.
To cancel or reduce both bearing forces and to achieve the desired independent motion in axial direction, the $\mathbf{M}_L$ matrix must fulfill the rank condition

$$\mathrm{rank}(\mathbf{M}_L) = 3. \qquad (22)$$

This implies a minimum number of three phases in order to generate the desired force and torque components $\mathbf{Q}$ and to fulfill the equation of motion (18). Thus, (13) must to be solved for $\mathbf{i}$, which results in

$$\mathbf{i}(\mathbf{q}) = \mathrm{inv}\left(\mathbf{M}_L(\mathbf{q})\right)\mathbf{Q}, \qquad (23)$$

where $\mathrm{inv}\left(\mathbf{M}_L\right)$ is a generalized matrix-inverse of $\mathbf{M}_L$.
For the given system the rank condition (22) is valid and thus the system (23) under-determined. Connecting the four phases in star reduces the number of degrees of freedom to three. Applying the phase connection matrix

$$\mathbf{V} = \begin{bmatrix} 1 & 0 & 0 \\ 0 & 1 & 0 \\ 0 & 0 & 1 \\ -1 & -1 & -1 \end{bmatrix} \qquad (24)$$

on (23) results in the new system

$$\mathbf{i}_c(\mathbf{q}) = \left(\mathbf{M}_L(\mathbf{q})\mathbf{V}\right)^{-1}\mathbf{Q} = \mathbf{K}_m(\mathbf{q})\mathbf{Q}, \qquad (25)$$

with $\mathbf{K}_m$ being the inverse of the quadratic matrix $\mathbf{M}_L\mathbf{V}$ and $\mathbf{i}_c$ the vector of the three independent phase currents of the star connected three phase system. The four individual coil currents

$$\mathbf{i} = \mathbf{V}\mathbf{i}_c \qquad (26)$$

can be calculated with the connection matrix $\mathbf{V}$.

B. Limits of bearing force reduction

From (25) follows that the compensation current required rises linear with the eccentricity and varies with the axial position. With the rated coil current as limit, the relative amount of bearing force compensation current required can be calculated for each phase. The simulation result of the bearing force compensation current in the absence of axial forces is given with respect to an equal eccentricity in both bearings and the axial position in Fig. 5. The simulation shows a moderate additional current demand as long as the eccentricities are within the typical range of manufacturing and assembling tolerances.

V. Experimental validation

A. Prototype setup

To validate the principle of bearing force reduction the prototype system in Fig. 7 has been manufactured. Stator and

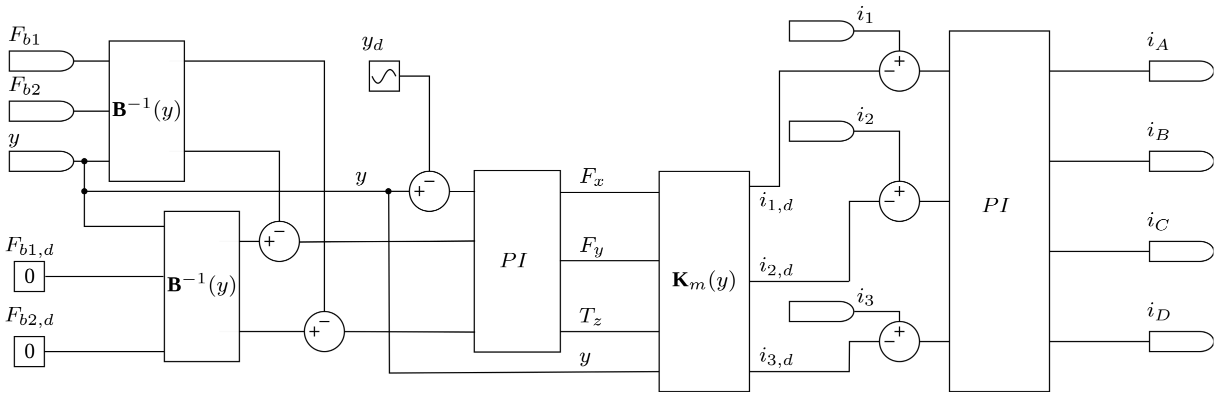

Figure 6. Control layout block diagram with the bearing force and phase current measurement as input. Block inputs labeled with a subscript 'd' indicate the demanded input values.

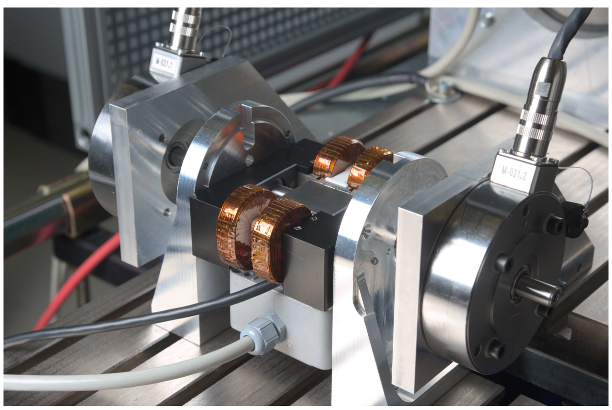

Figure 7. Prototype system at the test rig.

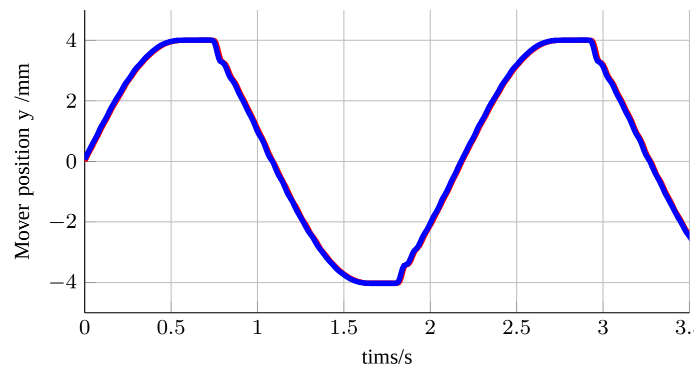

Figure 8. The uncompensated and compensated cases are measured under the same axial motion condition.

mover can be mounted independently from each other on the test rig to allow for an eccentricity and angular misalignment. The mover is attached to radial force load cells to measure the resulting bearing forces. The force compensation control itself is implemented on a TI microprocessor TMS320f28355 using the graphical software rapid prototyping tool X2C$^{\text{TM}}$[7]. A summary of the used measurement equipment is given in Tab. III.

Table III
MEASUREMENT EQUIPMENT.

Device	Type	Manufacturer
Radial force load cell	RK2	HBM
Amplifier	DAQP-CGB2	Dewetron
Power electronics and data acquisition unit	lcmEAse10HB10A	LCM
Axial position sensor	AS5311	AMS
Radial position sensor	eddy current	LCM

B. *Control system layout*

The control system's implementation bases on the force characteristics inversion given in (25). The actual bearing load forces F_{b1} and F_{b2} are measured, transformed to the mover's coordinate system using the inverse transformation given in (21). The resulting force in x-direction and the z-torque serve as feedback for the force compensation control loop. The force demand in y-direction, F_y, results from a position controller that performs for demonstration purposes a sinusoidal motion of the mover. All three force components are controlled using linear PI controllers. The output of the force control is transformed to the required phase currents as given in (25). An underlying PI current control for all three phases realizes a system with impressed currents. The control block diagram is given in Fig. 6.

C. *Measurements*

The prototype system is mounted to the test rig with an arbitrary position of the mover within the air-gap. The axial position of mover is controlled sinusoidally, what is given in Fig. 8. Clearly visible is the effect of the stick/slip friction. Even with the bearing force compensation applied the stick effect could not be removed. This may result from remaining bearing forces in the load cells in z-direction. The measured bearing forces for the compensated and uncompensated cases are given in Fig. 9 and the respective measured coils current in Fig. 10. The measurement proves that with the proposed method the bearing forces can be significantly reduced while the coil currents remain comparable.

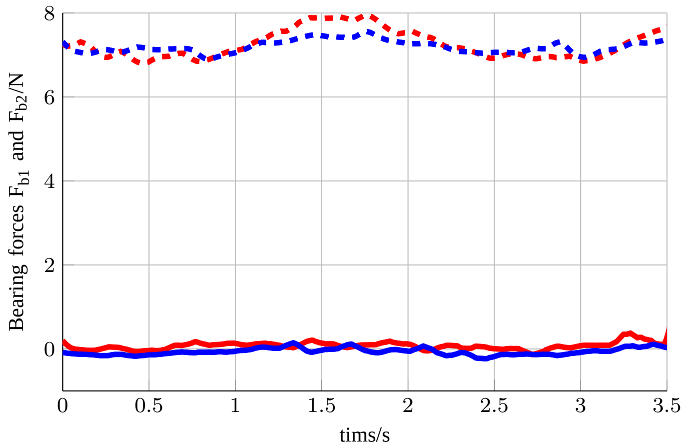

Figure 9. Measured bearing forces F_{b1} and F_{b2} of the uncompensated (dashed lines) and compensated (solid lines) system.

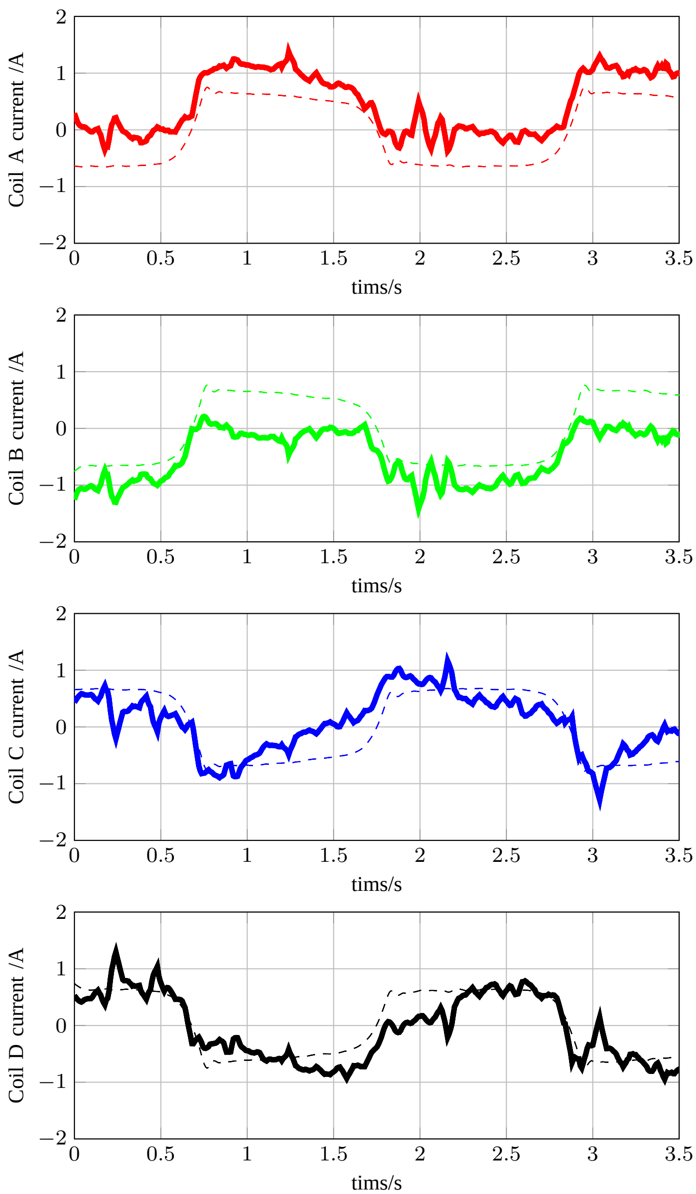

Figure 10. Measured coil currents of the uncompensated (dashed lines) and compensated (solid lines) system.

VI. Conclusion

The paper demonstrates the feasibility of reducing the unbalanced magnetic forces in PM linear actuators. The results are based on analytical and numerical methods and are validated by measurements. It is demonstrated that the bearing load can be reduced significantly and thus resulting in a longer lifetime regardless of the bearing material. While copper losses hardly increase, friction is eliminated almost completely. Using a closed loop control with force gauges allows completely eliminating any bearing forces as long as the system is operated within its magnetic and electrical limits.

References

[1] A. J. P. Ortega and L. Xu, “Investigation of effects of asymmetries on the performance of permanent magnet synchronous machines,” *IEEE Transactions on Energy Conversion*, vol. 32, no. 3, pp. 1002–1011, Sept 2017.

[2] J. J. H. Paulides, J. L. G. Janssen, and E. A. Lomonova, “Bearing lifetime of linear pm machines,” in *Energy Conversion Congress and Exposition, 2009. ECCE 2009. IEEE*, 2009, pp. 1083–1090.

[3] Nan-Chyuan Tsai and Chao-Wen Chiang, “High-frequency linear compressor and lateral position regulation,” *Control Systems Technology, IEEE Transactions on*, vol. 20, no. 1, pp. 127–138, 2012.

[4] Shi-Uk Chung, Ji-Won Kim, Byung-Chul Woo, Do-Kwan Hong, Ji-Young Lee, and Dae-Hyun Koo, “Force ripple and magnetic unbalance reduction design for doubly salient permanent magnet linear synchronous motor,” *Magnetics, IEEE Transactions on*, vol. 47, no. 10, pp. 4207–4210, 2011.

[5] T. T. Nguyen, H. Butler, and M. Lazar, “An analytical commutation law for parasitic forces and torques compensation in coreless linear motors,” in *2016 European Control Conference (ECC)*, 2016, pp. 2386–2391.

[6] F. Poltschak, “Active bearing force reduction in non-commutated linear actuators,” *Proceedings of the Institution of Mechanical Engineers, Part I: Journal of Systems and Control Engineering*, vol. 230, no. 4, pp. 352–360, 2016.

[7] LCM, “X2C - a free and open source tool for the model-based development and code generation of real time control algorithms for micro processor units,” accessed: June 2018. [Online]. Available: http://www.mechatronic-simulation.org/